# Ground states of one-dimensional commensurate-incommensurate transition models with double-well interactions

Aiguo Xu*
*CCAST (World Laboratory), P. O. Box 8730, Beijing, 100080, People's Republic of China;*
*Graduate School, China Academy of Engineering Physics, P.O. Box 8009-30, Beijing, 100088, People's Republic of China;*
*and International Center for Materials Physics, Academia Sinica, Shenyang, 110015, People's Republic of China*

Guangrui Wang* and Shigang Chen*
*Center for Nonlinear Studies, Institute of Applied Physics and Computational Mathematics, P.O. Box 8009-28, Beijing 100088, People's Republic of China*

Bambi Hu
*Department of Physics and Center for Nonlinear and Complex Systems, Hong Kong Baptist University, Kowloon Tong, Hong Kong*
*and Department of Physics, University of Houston, Houston, Texas 77204*
(Received 5 March 1997)

Multiwell interparticle potentials are proposed as a mechanism for the occurrence of modulated phases. This is examined through two models with double-well interactions. For these systems, the effective potential method is reviewed and a certain process of calculation is emphasized. To characterize the modulated phases, the winding number $\omega$, and the rotation number $\Omega$ are redefined. The method to recover the chain of particles and calculate the value of $\omega$ is given. We find that the phase diagrams strongly relate to the period of the external potential $D$. For each model, there is a threshold value in $D$, which equals to the distance between the two minimum value points. Within different interval of $D$, the phase diagrams exhibit different behavior. The periodicity of the phase diagram and the difference between modulated phases with the same $\Omega$ are also discussed. [S0163-1829(98)01805-0]

## I. INTRODUCTION

When a system possesses two or more length scales, a type of complicated phase transition, called commensurate-incommensurate (CI) phase transition, can occur. CI transitions have been observed in many real systems such as some spin-density-wave (SDW) systems, e.g., cerium antimonide; charge-density-wave (CDW) systems, e.g., tetrathiofulvalene tetracyano-p-quinodimethane (TTF-TCNQ), and $K_2P_t(CN)_4Br_{0.30}3H_2O$ (KCP), magnetic spirals and absorbed monolayers.[1] In order to understand the modulated structure of the ground states and the rules of CI transition, a variety of phenomenological models have been proposed to describe such systems. One of the simplest models of this type is the ground state of an infinite one-dimensional system of particles (or classical spins) with energy

$$H=\sum [V(U_n)+W(U_{n+1}-U_n)], \tag{1}$$

where $U_n$ is the position of the $n$th particle in the chain (or the angle between the spin vector at the $n$th site and the applied field). The most famous model of this type is perhaps the Frenkel-Kontorova[2] (FK) model, which describes a chain of atoms connected by harmonic springs in the presence of a sinusoidal external potential. The ground states of the FK-like models can be precisely determined using the gradient method[3] when the interparticle interactions are convex. Because of the correspondences of the ground states and orbits of the two-dimensional area-preserving map, we can transcribe many results of the map to those of the model. The FK-like models of this type have been extensively studied by Aubry,[3] Coppersmith,[4] Biham,[5] and Hu and co-workers.[6]

However, nonconvex interactions are very common in solid state physics. The oscillating exchange interaction between localized spins in a metal is perhaps the most famous example. Also, the magnetoelastic coupling leads to an effective double-well interparticle interaction.[7] More generally, and relevant to ferroelectricity, oscillating (and hence nonconvex) interactions can be mediated through elastic strains and other harmonic fields.[8] Little and Zangwill[9] also introduce a Frenkel-Kontorova-Devonshire (FKD) model where as a function of a single parameter (which is regarded as the temperature), the interparticle potential changes smoothly from a quadratic single well to symmetric triple well and finally to a symmetric double well. Models describing systems of spins were studied by Banerjea and Taylor[10] and Yokoi.[11] Some universals have been found. Up to now, we know very little about the models (such as atomic systems, not the systems of spins) of this type with nonconvex interparticle interactions, though Griffiths and Chou,[12] Marchand,[13] had made some attempts. In this paper, we devote to this kind of study through two two microscopic models with double-well interactions.

We present the results of our studies in eight sections. In Sec. II we introduce the two models and analyze the foundmental properties of the ground states that are universal in the KF-like models. In Sec. III, we present a brief review of the effective potential method for these systems of particles (not the systems of spins). The winding number $\omega$ and the rotation number $\Omega$ are defined in this section. An impor-

 

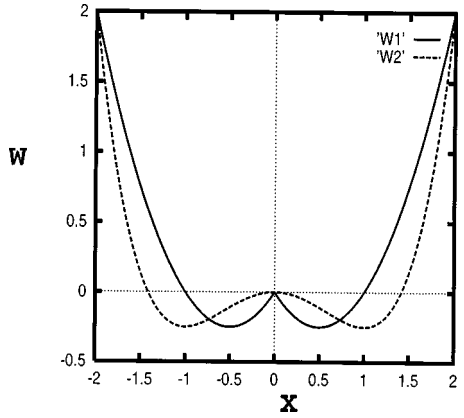


FIG. 1. The interparticle interaction potentials of the two models. The solid line denotes $W(x)$ for model 1 and the dashed line denotes $W(x)$ for model 2, where $\gamma=0$.

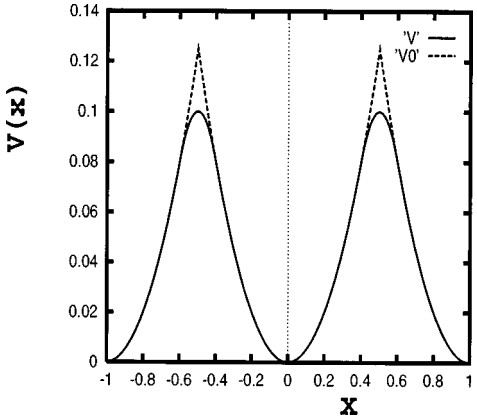


FIG. 2. The curve of the external potential $V(x)$ with $K=1$. The dashed line corresponds to the case of $\Delta=0$ and the solid line corresponds to the case of $\Delta=0.1$.

tant process in the numerical calculation is explained and emphasized. In Sec. IV we discuss the periodicity of the phase diagram and the difference between modulated phases with the same rotation number. The method to recover the chain of particles and calculate the winding number $\omega$ is given in Sec. V. The phase diagram of model 1 is studied in Sec. VI and the phase diagram of model 2 is studied in Sec. VII. Section VIII is the summary and conclusion. From our study, one can clearly find that there are many nonconvex phase, where the numerator and the denominator have a common divisor, and some multiphase points in the $(K,\gamma)$ spaces for the two models.

## II. ANALYSIS OF THE MODELS

The interparticle potentials[14] of the two models used in this paper are

$$W(x)=(x-\gamma)^2-|x-\gamma| \quad \text{(model 1)}, \tag{2}$$

$$W(x)=-\tfrac{1}{2}(x-\gamma)^2+\tfrac{1}{4}(x-\gamma)^4 \quad \text{(model 2)}, \tag{3}$$

respectively. The most significant difference between these two models is the fact that the region of nonconvexity of $W(x)$ is of finite width ($|x-\gamma|<3^{-1/2}$) in model 2, whereas it is limited to the nonanalytic point $x=\gamma$ in model 1. The curves of $W(x)$ for the two models are shown in Fig. 1, where $\gamma=0$, the solid line is for model 1 and the dashed line is for model 2. $W(x)$ has two equal minimum values that locate $x-\gamma=\pm\gamma_1=\pm 0.5$ for model 1, and it has two equal minimum values that locate $x-\gamma=\pm\gamma_2=\pm 1$ for model 2. The external potential used in this paper is

$$V(x)=\begin{cases}\dfrac{1}{2}K\left(\dfrac{D}{2}-\Delta\right)^2+\dfrac{K(D/2-\Delta)\Delta}{2}-\dfrac{K(D/2-\Delta)}{2\Delta}\left(x+\dfrac{D}{2}\right)^2, & -\dfrac{D}{2}<x\leqslant-\dfrac{D}{2}+\Delta\\[2ex] \dfrac{1}{2}Kx^2, & -\dfrac{D}{2}+\Delta<x\leqslant\dfrac{D}{2}-\Delta\\[2ex] \dfrac{1}{2}K\left(\dfrac{D}{2}-\Delta\right)^2+\dfrac{K(D/2-\Delta)\Delta}{2}-\dfrac{K(D/2-\Delta)}{2\Delta}\left(x-\dfrac{D}{2}\right)^2, & \dfrac{D}{2}-\Delta<x\leqslant\dfrac{D}{2}.\end{cases} \tag{4}$$

The curve of $V(x)$ is shown in Fig. 2, where $D=1$; the solid line corresponds to $\Delta=0.1$ and the dashed line corresponds to $\Delta=0$.

Under the minimum-enthalpy condition[12], $W$ in Eq. (1) can be replaced by $W^*$, where $W^*(x)=\min_m W(x+mD)$, and $m$ is a arbitary integer that satisfies a certain condition. Hence $W^*$ is periodic in a certain direction and the period is just that of the external potential. For model 1, the curve of $W$ in the interval $-1\leqslant x-\gamma\leqslant 0$ is just identical to that in the interval $0\leqslant x-\gamma\leqslant 1$, so the curve of $W^*$ with $D=1$ is just the same as that with $D=2$. This feature is very useful in the understanding of Fig. 4 and Fig. 5(d).

From Ref. 13 and the references therein we know that, for Hamiltonians of the type given by Eq. (1) having $V(-x)=V(x)$, a nondegenerate ground state of even period $Q$ must have the following structure (over one period):

$$\{U_n\}=\{-U_Q,-U_{Q-1},\ldots,-U_{Q/2+1},U_{Q/2+1},\ldots,U_{Q-1},U_Q\} \tag{5}$$

with all $U_n \neq 0$, whereas a nondegenerate ground states of odd period $Q$ must have the form

$$\{U_n\}=\{-U_Q,-U_{Q-1},\ldots,U_{(Q+1)/2},\ldots,U_{Q-1},U_Q\} \tag{6}$$

with all $U_n \neq 0$ except for $U_{(Q+1)/2}=0$. That is to say, the particles in the ground states distribute symmetrically with respect to the origin point, and have no dislocation phenomenon (i.e., $U_{n-1}>U_n$) occur. This property can also be understood in the following way: In the chain of particles described by Eq. (1), if the position of the $(n-1)$th and the position of the $n$th particles are exchanged, then the original $n$th particle becomes the $(n-1)$th one and the original $(n-1)$th one become the $n$th one. Because all the particles in the chain are identical, the new chain of particles is just the same as the old one. That is to say, no dislocation occurs. This property is very useful in distinguishing the correct algorithm of calculating the effective potential from the wrong one.

## III. REVIEW OF THE EFFECTIVE POTENTIAL METHOD; THE WINDING NUMBER AND ROTATION NUMBER

In order to continue our analysis, we give a brief review of the effective potential method[12] for the kind of systems we are studying.

Imagine that a system described by Eq. (1) is in its ground state. If we displace a particle from its equilibrium position, then the surrounding paricles will change their positions to minimize the total energy. This local deformation will, in general, cost some energy and therefore, we can define a function, called the *effective potential*, which will describe this energy cost as a function of the particle's position. At site $n$, the effective potential $R(U_n)$, due to the presence of the particles $i<n$, can be formally written as

$$R(U_n)\equiv\min_{i<n}\left\{\sum_{i\leqslant n}[W(U_i-U_{i-1})+V(U_i)-\lambda]\right\}, \tag{7}$$

where $\lambda$ is the (unknown) ground-state energy per particle and where the minimum must be taken over all particles' positions $U_i$ with $i<n$. We can rewrite this equation by expressing the right-hand side (RHS) in terms of $R(U_{n-1})$ and, in this manner, we obtain the following nonlinear eigenvalue equation:

$$\lambda+R(U_n)=V(U_n)+\min_{U_{n-1}}\{W(U_n-U_{n-1})+R(U_{n-1})\}. \tag{8}$$

The RHS of Eq. (8) defines a nonlinear functional operator Re and Eq. (8) can be rewritten simply as

$$\lambda+R(U_n)=\mathrm{Re}\ R(U_n). \tag{9}$$

We can also write the effective potential $S(U_n)$ due to the presence of the particles $i>n$ as

$$S(U_n)\equiv\min_{i>n}\left\{\sum_{i\geqslant n}[W(U_{i+1}-U_i)+V(U_i)-\lambda]\right\} \tag{10}$$

and the associated eigenvalue equation is

$$\lambda+S(U_n)=V(U_n)+\min_{U_{n+1}}\{W(U_{n+1}-U_n)+S(U_{n+1})\}. \tag{11}$$

Hence the total effective potential $F(U)$, due to all the neighboring particles, is given by

$$F(U)=R(U)+S(U)-V(U), \tag{12}$$

where $V(U)$ is substracted to aviod being counted twice. When $V(-U)=V(U)$, comparison of Eqs. (8) and (11) yields

$$S(U)=R(-U) \tag{13}$$

and hence, in this case, all the information is contained in $R(U)$.

For a given value of $U_n$, the value of $U_{n-1}$ that minimizes the RHS of Eq. (8) defines the one-dimensional (1D) map,

$$U_{n-1}=\rho(U_n). \tag{14}$$

Similarly, for a given $U_n$, the value of $U_{n+1}$ that minimizes the RHS of Eq. (11) defines the 1D map,

$$U_{n+1}=\sigma(U_n). \tag{15}$$

Physically we expect that, after some initial transient behavior, the orbits of $\rho$ and $\sigma$ will tend to an attractor that represents the ground state. Hence, to generate the ground state, we only need to iterate $\rho$ or $\sigma$ once we have obtained $R(U)$ or $S(U)$.

We are usually unable to find an analytic solution to Eq. (8) and need to rely on numerical solutions. Because the effective potentials $R(U)$, $S(U)$, and $F(U)$ have the same period as that of $V(U)$, we can calculate the values of $R(u_n)$, $S(u_n)$, $F(u_n)$, and $V(u_n)$, instead of $R(U_n)$, $S(U_n)$, $F(U_n)$, and $V(U_n)$, where $u_n$ denote the displacement of the $n$th particle with respect to some reference position, here is a regular one-dimensional lattice of equally spaced points. One way to proceed is to discretize the unit cell. We replace the continuous set of possible particles' positions by a discrete set of $G$ points uniformly spaced on an interval $D$, which is the period of the external potential: $u_i=-(D/2)+i(D/G)$ with $i=1,2,\ldots,G$. Choosing $R^0(u)=V(u)$ as the trial function, the sequece of iterations,

$$R^{j+1}(u)=\tfrac{1}{2}[\mathrm{Re}\ R^j(u)+R^j(u)]-C_j, \tag{16}$$

generally converges. The constant $C_j$ is chosen in order that the minimum value of $R^{j+1}(u)$ be zero. This sequece is iterated until

$$\max_u|\mathrm{Re}\ R^j(u)-\lambda^j-R^j(u)|<\epsilon\max_u|R^j(u)|, \tag{17}$$

where the approximate ground-state energy is given by

$$\lambda^j=\min_u\{\mathrm{Re}\ R^j(u)\} \tag{18}$$

and the final $R^j(u)$ is the approximate effective potential.

In the numerical calculation, the method to calculate the $\mathrm{Re}R(u_n)$ should be emphasized. According to Sec. II, no dislocation occurs in the ground states, so the coordinate of

the $n$th particle should be greater than that of the $(n-1)$th particle, i.e., $U_n > U_{n-1}$. In the process of calculation, $u_{n-1} < u_n$ means that, for a given $U_n = u_n$, the possible positions of the $(n-1)$th particle should be $U_{n-1} = u_{n-1} - m_{n-1}D$, where $m_{n-1}$ is a certain *non-negative* integer. In this case, $W(U_n - U_{n-1}) = W^*(u_n - u_{n-1})$ should take $W(u_n - (u_{n-1} - m_{n-1}D))$, which is the minimum value of $W(u_n - u_{n-1})$, $W(u_n - u_{n-1} + D)$, $W(u_n - u_{n-1} + 2D)$, .... $u_{n-1} > u_n$ means that, for a given $U_n = u_n$, the possible positions of the $(n-1)$th particle should be $U_{n-1} = u_{n-1} - m_{n-1}D$, where $m$ is a certain *positive* integer. In this case, $W(U_n - U_{n-1}) = W^*(u_n - u_{n-1})$ should take $W(u_n - (u_{n-1} - m_{n-1}D))$, which is the minimum value of $W(u_n - u_{n-1} + D)$, $W(u_n - u_{n-1} + 2D)$, $W(u_n - u_{n-1} + 3D)$, ... .

When $W(x)$ is a convex function or a nonconvex multiwell function with only one absolute minimum value, the value of $\min_m\{W(u_n - u_{n-1} + mD)\}$ is unique, where $m$ is a arbitary *non-negative* integer for the case of $u_n > u_{n-1}$ and is a arbitary *positive* integer for the case of $u_{n-1} > u_n$. There is no degeneration in ground states no matter whether $V \equiv 0$ or $V > 0$. When $W(x)$ is a multiwell potential function with more than one absolute minimum value, the value of $\min_m\{W(u_n - u_{n-1} + mD)\}$ is not unique. When $V \equiv 0$, for a given $U_n = u_n$, there would be more than one position for the $(n-1)$th particle to occupy. In this case, the degeneration occurs.

To characterize the modulted phase more precisely, we define two parameters as follows: First define the winding number

$$\omega = P/Q,$$

where $Q$ is the period of the ground state and $P$ is the period number of the external potential between the 1st and the $(Q+1)$th particles. One can find that when $W$ is a convex function everywhere, this definition is equivalent to the traditional definition of the winding number. Next define the rotation number

$$\Omega = \frac{1}{Q}\sum_{n=1}^{Q} \Theta(u_{n-1} - u_n),$$

where $Q$ is the period of the ground state, $u_Q = u_0$, and $\Theta(x) = +1$ (if $x \geqslant 0$) and $\Theta(x) = 0$ (if $x < 0$). In the following sections, one can find that $\omega = \Omega$ in some cases and $\omega \neq \Omega$ in other cases. The coorperation of the the two parameters can present more information about the ground states.

Figure 3 gives an example of variance of $F(U)$ with $\Delta$ for model 2, where $D = 1$, $K = 1$, $\gamma = 1.4$, and where $FU0$, $FU1$, $FU2$, $FU3$, $FU4$ correspond to the cases of $\Delta = 0$, 0.05, 0.1, 0.2, 0.3, respectively. In the five cases, the values of $\Omega$ are all just 2/5. It is clear from Fig. 3 that $\Delta$ only affect the boundary region of $F(U)$ when $\Delta$ is small, but it affects the whole region of $F(U)$ when it is large enough. Generally, the value of $\Delta$ may also affect the value of $\Omega$. In the following calculations, the value of $\Delta$ is limited to be small enough so that it only affects the boundary region of $F(U)$ and does not affect the positions of the particles in the ground state.

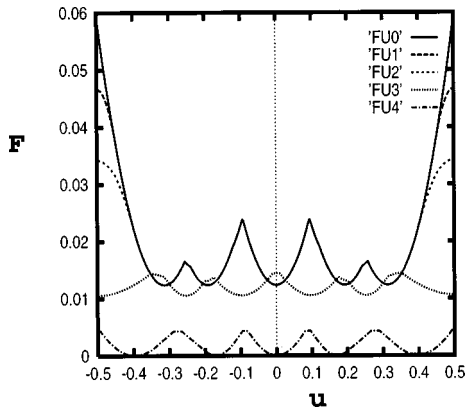


FIG. 3. Examples of the variance of $F(U)$ with $\Delta$, where $D = 1$, $K = 1$, $\gamma = 1.4$, $G = 400$, and $\epsilon = 1 \times 10^{-5}$, and where $FU0$, $FU1$, $FU2$, $FU3$, and $FU4$ correspond to the cases of $\Delta = 0$, 0.05, 0.1, 0.2, and 0.3, respectively.

## IV. PERIODICITY OF THE PHASE DIAGRAM; THE DIFFERENCE BETWEEN MODULATED PHASES WITH THE SAME ROTATION NUMBER

In order to study the periodicity of the phase diagrams for the two models, we first consider that of the standard FK model.

For the standard FK model, the winding number $\omega$ equals to the nature length of the harmonic spring $\gamma$ when the strength of the external potential is zero. In this case, for a given $\gamma = \gamma_0 \in [0, D]$, $\omega = \Omega = P/Q = \gamma_0/D$, where we assume $D$ is the period of the external potential. When $\gamma = D + \gamma_0$, $\omega = 1 + P/Q$, and $\Omega = P/Q$. When the strength of the external potential is greater than zero, we have the same conclusion. If we only use the rotation number $\Omega$ to describe the phases, the phase diagram is periodic and the period is just the same as that of the external potential. Because no degeneration occurs, the winding number $\omega$ can uniquely characterize each tongue of the phase diagram.

For the present model 1 (or model 2), when $\gamma \geqslant \gamma_1$ (or $\gamma \geqslant \gamma_2$), $W(x)$ can take any one of the two equal minimum values, and $W^*(x)$ is periodic in a certain direction. So if we only use the rotation number $\Omega$ to describe phases, the phase diagram is also periodic, and the period is just the same as that of the external potential. If $\Omega = \Omega_0$ and $\omega = \omega_0$ when $\gamma = \gamma_0$, then $\Omega = \Omega_0$ and $\omega = 1 + \omega_0$ when $\gamma = D + \gamma_0$. When $\gamma < \gamma_1$ (or $\gamma < \gamma_2$), $W(x)$ cannot take its left minimum value, so the phase diagram may be very different.

From the above analysis, one can easily find that modulated phases with the same rotation number may have different winding numbers, and thus may correspond to different phase structures [see Fig. 4 for an example]. If $W(x)$ is a convex function everywhere, then $\omega = m + \Omega$, where $m$ is a appropriate non-negative integer. If $W(x)$ is nonconvex, the relation between $\omega$ and $\Omega$ is much more complex, although there are rules to obey. The numerical results in Sec. VI and Sec. VII support our analysis and give examples.

## V. METHOD FOR RECOVERING THE CHAIN OF PARTICLES AND CALCULATING THE WINDING NUMBER

When we use the effective potential method to study the ground states, all the $u_n$ are contained in the intervals

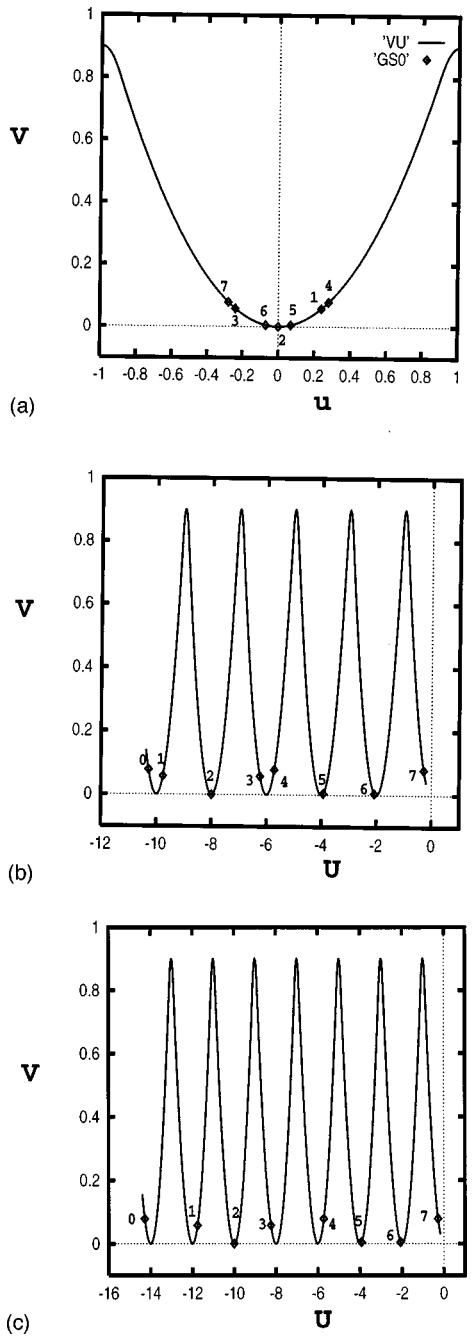


FIG. 4. Examples of the ground states for model 1, where $\diamond$ denotes particle and $\gamma \geqslant 0.5$. (a) shows the ground state $\{u_n\}$, where $D=2$, $K=2$, $\gamma=1.2$ (or $\gamma=2.2$), and $\Omega=5/7$; (b) shows the recovered chain of particles where $\gamma=1.2$ and $\omega=\Omega=5/7$; (c) shows the recovered chain of particles where $\gamma=2.2$ and $\Omega=5/7$, $\omega=7/7$.

$[-D/2,D/2]$, which do not denote the real positions of the particles in the chain. We can recover the chain of particles in the following way: Once we have obtained the effective potential $R(u)$, then in the process of calculating the ground state, more precisely, in the process of calculating $\mathrm{Re}\, R(u_n)$, for a given $U_n=u_n$, we should record the period number of the external potential, assumed to be $m_{n-1}$, which should be moved to the left from $u_{n-1}$ to obtain $U_{n-1}$. Thus for a ground state of $\Omega=P/Q$, assume that $U_Q=u_Q$, then $U_{Q-1}=u_{Q-1}-m_{Q-1}D$, $U_{Q-2}=u_{Q-2}-(m_{Q-1}+m_{Q-2})D$, $\ldots$, $U_1=u_1-(m_{Q-1}+m_{Q-2}+\cdots+m_1)D$, $U_0=u_0-(m_{Q-1}+m_{Q-2}+\cdots+m_1+m_0)D$, where $u_0=u_Q$ and $\omega=P/Q\equiv(m_{Q-1}+m_{Q-2}+\cdots+m_0)/Q$. Figures 4(a)–4(c) show examples of ground states for model 1, where the $\diamond$ denotes the particle. Figure 4(a) shows the ground state $\{u_n\}$ when $D=2$, $K=2.0$, $\gamma=1.2$ (or $\gamma=2.2$), $\Omega=5/7$. All the particles in one period of the ground state have been plotted in one well of the external potential, and do not denote the real positions of the particles. Figure 4(b) shows the recovered chain from Fig. 4(a) in one period where $\gamma=1.2$, $\Omega=\omega=5/7$. Figure 4(c) shows the recovered chain from Fig. 4(a) in one period where $\gamma=2.2$, $\Omega=5/7$, and $\omega=7/7$. One can find that two different ground states correspond to the same unrecovered chain; we have numerically proven that the energies of the two phases are unequal.

## VI. THE PHASE DIAGRAMS OF MODEL 1

Figures 5(a)–5(e) show the examples of the phase diagrams of model 1 in the case of $\gamma \geqslant \gamma_1$, where the external potential period are $D=\gamma_1$, $2\gamma_1$, $3\gamma_1$, $4\gamma_1$, $5\gamma_1$, respectively. Here, only the phases with $Q \leqslant 5$ are shown. The rotation numbers are $\Omega=1/1$, 1/5, 1/4, 1/3, 2/5, 1/2, 3/5, 3/4, 4/5, 1/1, respectively. From Figs. 5(a)–5(b) it is clear that the phase diagram with $D=0.5$ or $D=1$ is similar in appearance to that of the standard FK model, which is composed of commensurate and incommensurate ground states in the $(K,\gamma)$ parameter space. For any given rotation number $\Omega$, there is a corresponding commensurate area (Arnold's tongue) in which $\Omega$ is a constant. Between any two tongues there is a gap that contains incommensurate states as well as higher-order commensurate states. But in fact the phase structures may be greatly different from that of the standard FK model. For the standard FK model, with the increasing of $\gamma$, the values of $\Omega$ occur periodically and conform to the structure of the Farey tree except for the case of $Q=1$; the values of $\omega$ increase monotonically. For model 1, with the increasing of $\gamma$, the values of $\Omega$ occur periodically and conform to the structure of Farey tree except for the case of $Q=1$, but the values of $\omega$ do not increase monotonically. In Fig. 5(a), from left to right, the winding numbers are $\omega=2/1$, 11/5, 3/4, 7/3, 12/5, 5/2, 13/5, 4/3, 9/4, 14/5, 4/1, respectively. In Fig. 5(b), from left to right, the winding numbers are $\omega=1/1$, 6/5, 7/4, 3/3, 8/5, 3/2, 6/5, 3/3, 7/4, 8/5, 3/1, respectively. The period of the phase diagram for model 1 with $D=0.5$ or $D=1$ is just the same as that of the external potential.

From Figs. 5(c)–5(e), one can find that, among the commensurate tongues, the structure of the Farey tree occurs two times within one period of the external potential. The fraction numbers labeled in the figure are the values of $\Omega$ of the corresponding tongues. One also can find that in Figs. 5(c)–5(e) the $(K,\gamma)$ parameter space is divided into two unequivalent parts, which cover the regions of $A_1$, $\gamma_1 \leqslant \gamma \leqslant (D-\gamma_1)$; and $A_2$, $(D-\gamma_1) \leqslant \gamma \leqslant (D+\gamma_1)$, respectively. The phase diagrams in the two parts are both similar to that of the standard FK model. In the leftmost region of uniform phase, $\Omega=1/1$ and $\omega=0/1$. In the other tongues of the left part, $\omega=\Omega$. In the right part the phase diagram is identical to that in the case of $\gamma \geqslant \gamma_1$ and $D=2\gamma_1$, but within the tongue with $\Omega=P/Q$, the winding number $\omega=Q/Q$.

When $D=\gamma_1$ and $0 \leqslant \gamma \leqslant \gamma_1$, the phase diagram is just the

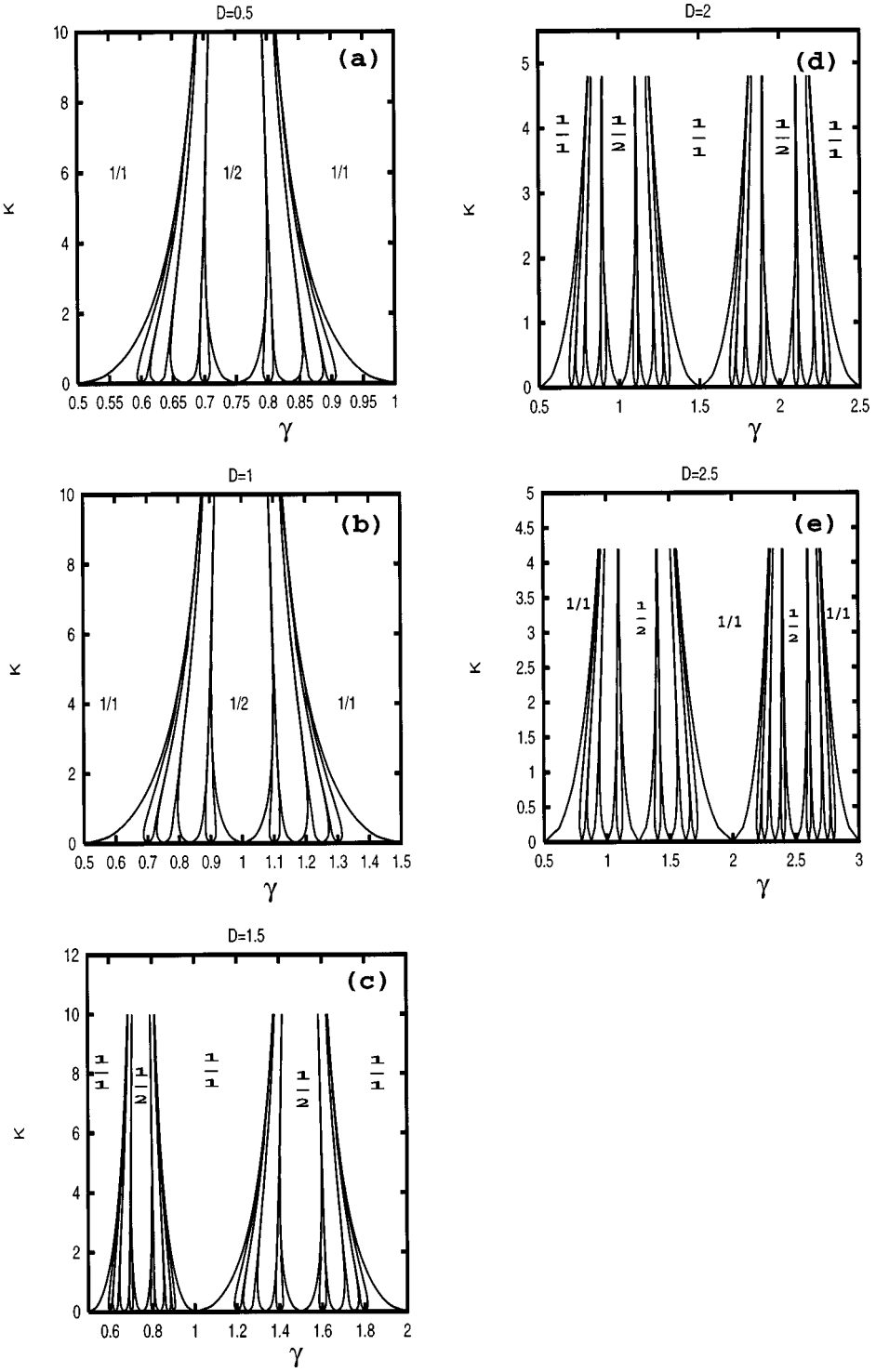


FIG. 5. Phase diagrams of model 1. (a), (b), (c), (d), and (e) correspond to the cases of $D=0.5$, $D=1$, $D=1.5$, $D=2$, and $D=2.5$, respectively, where only the phases with the period $Q\leqslant 5$ are shown. The fraction numbers labeled in the figures are the rotation numbers of the corresponding tongues.

same as that of the case when $D=\gamma_1$ and $\gamma_1\leqslant\gamma\leqslant 2\gamma_1$ in appearance, but where $\omega=1+\Omega$ except for the left uniform phase. In the region of the left uniform phase, $\omega=\Omega=1/1$.

## VII. THE PHASE DIAGRAMS OF MODEL 2

Figures 6(a)–6(e) give the examples of phase diagrams of model 2 in the case of $\gamma\geqslant\gamma_2$, where only the phases with $Q\leqslant 5$ are shown, and where the values of $D$ are $\gamma_2$, $2\gamma_2$, $2.5\gamma_2$, $4\gamma_2$, $5\gamma_2$, respectively. The phase diagram with $D=\gamma_2$ is an example of the cases that $D<2\gamma_2$, which is similar to that of the standard FK model. When $1\leqslant\gamma<2$, from left to right, the rotation numbers are $\Omega=1/1$, 1/5, 1/4, 1/3, 2/5, 1/2, 3/5, 2/3, 3/4, 4/5, 1/1, respectively. The corresponding winding numbers are $\omega=2/1$, 9/5, 7/4, 5/3, 8/5, 3/2, 9/5, 4/3, 5/4, 10/5, 1/1, respectively, when $\gamma=2$, $\Omega=1/1$, $\omega=4/1$.

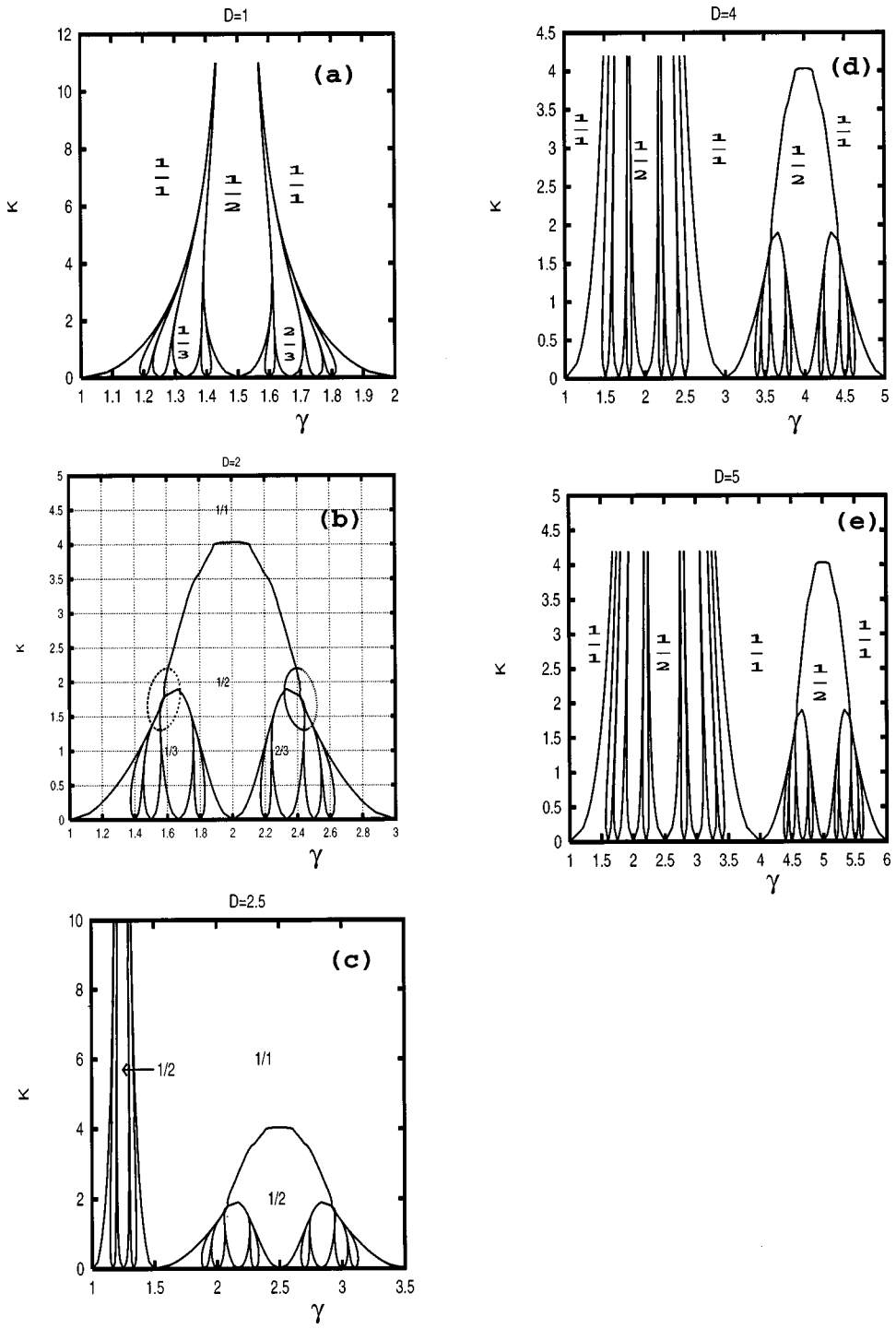


FIG. 6. Phase diagrams of model 2, where only the phases with the period $Q \leqslant 5$ are shown. The fraction numbers labeled in the figures are the rotation numbers of the corresponding tongues. (a), (b), (c), (d), and (e) correspond to the cases of $D=1$, $D=2$, $D=2.5$, $D=4$, and $D=5$, respectively, where $\gamma \geqslant \gamma_2$; (f) and (g) correspond to the cases of $D=1$ and $D=2$, respectively, where $\gamma \leqslant \gamma_2$.

The phase diagram with $D=2\gamma_2$ is very different from that of the standard FK model. In Fig. 6(b), most of the phase space is occupied by the uniform phase and all the phases with $Q>1$ vanish when $K$ is greater than a threshold value $K_c$, which is approximately 4.0. In the region limited by the left dashed ellipses there is a typical multiphase point,[13] around which we found the following phases: $\Omega=1/1$, 1/4, 1/3, 1/2, 2/4, respectively. The corresponding winding numbers are $\omega=1/1$, 4/4, 3/3, 2/2, 4/4, respectively. In the region limited by the right dashed ellipses there is also a typical multiphase point, around which we found the following phases: $\Omega=1/1$, 3/4, 2/3, 1/2, 2/4, respectively. The corresponding winding numbers are $\omega=1/1$, 4/4, 3/3, 4/4, respectively. In the region of uniform phase, $\Omega=1/1$, $\omega=1/1$. Our numerical results show that in this region of the parameter $\gamma$, an interesting phenomenon occurs. The winding number $\omega = Q/Q$ when $\Omega = P/Q$.

In Figs. 6(c)–6(e), a more interesting phenomenon occurs. The $(K,\gamma)$ parameter space is divided into two unequivalent parts. The phase diagram in the left part is similar to that in

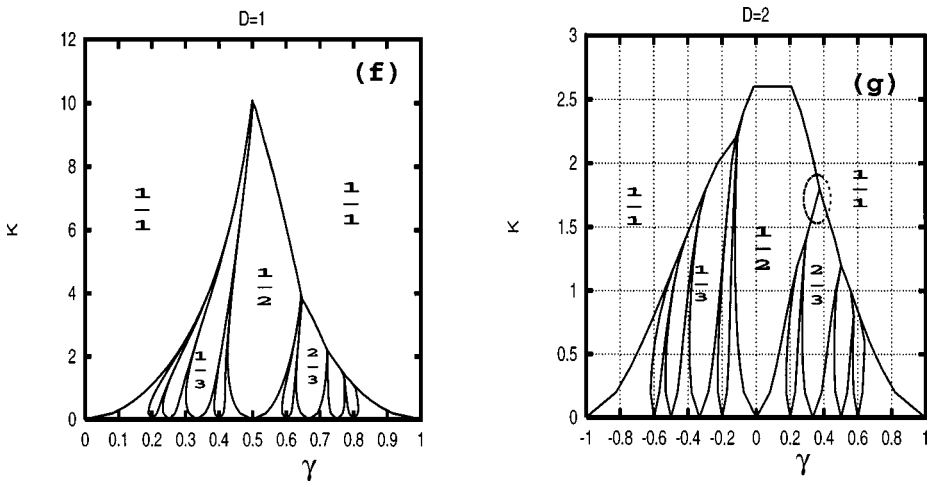


FIG. 6. (*Continued*).

the case of $\gamma \geqslant \gamma_2$ and $D<2\gamma_2$, it covers the region $B_1$: $\gamma_2 \leqslant \gamma \leqslant D-\gamma_2$. In the leftmost regions of uniform phase in Fig. 6(c), Fig. 6(d), or Fig. 6(e), $\omega=0/1$, and $\Omega=1/1$. Within the other tongues in the left part, $\omega=\Omega$. The phase diagram in the right part is identical to that in the case of $\gamma \geqslant \gamma_2$ and $D=2\gamma_2$. Within a given tongue in the right part, the winding number and the rotation number are just the same as those in the case of $D=2\gamma_2$, it covers the region $D-\gamma_2 \leqslant \gamma \leqslant D+\gamma_2$. Unlike model 1, the phase diagrams in the two parts are very different.

Figures 6(f)–6(g) give examples of phase diagrams when $\gamma<\gamma_2$. The interparticle interaction $W(x)$ cannot take its left minimum value. The phase diagrams in Fig. 6(f) or Fig. 6(g) are not periodic. In Fig. 6(f), all the phases with $Q>1$ disappear when $K$ is greater than a certain threshold value $K_c$, where $K_c$ is approximately 10. In this region of the parameter $\gamma$, $\omega=\Omega$ except for the uniform phase. In the region of uniform phase, $\omega=\Omega=1/1$ when $0 \leqslant \gamma<0.5$; $\omega=0/1$ and $\Omega=1/1$ when $0.5<\gamma<1$; $\omega=2/1$ and $\Omega=1/1$ when $\gamma=1$. There are obviously many multiphase points in this figure. One locates on the top of the tongue with $\Omega=1/2$, the others locate on the top of tongues with $\Omega>1/2$, respectively. In Fig. 6(g), all the phases with $Q>1$ disappear when $K>K_c$, where $K_c$ is approximately 2.6. In this region of the parameter $\gamma$, $\omega=\Omega$, except for the case of the uniform phase. In the region of uniform phase, $\omega=0/1$, $\Omega=1/1$. In the region limited in the dashed line ellipse, we also find a multiphase point and the phase with $\Omega=\omega=2/4$.

## VIII. SUMMARY AND CONCLUSION

We study two models with double-well interparticle potentials. For the convenience of studying, we review the effective potential method for the systems of particles (not the systems of spins). To characterize the modulated phases, we redefine two parameters, the winding number $\omega$ and the rotation number $\Omega$, which are equivalent to the traditional definition of the winding number under some conditions. The cooperation of the two parameters can give more information about the modulated phases, so can more precisely determine the structures of the ground states. Because the two models have the double-well interparticle interactions, the nonconvex phase and multiphase points may appear. For the two models, when $\gamma \geqslant \gamma_1$ (for model 1) or $\gamma \geqslant \gamma_2$ (for model 2), $W(x)$ can take any one of the two equal minimum values, the phase diagram is periodic and the period is just the same as that of the external potential. If $\Omega=\Omega_0$ and $\omega=\omega_0$ when $\gamma=\gamma_0$, then $\Omega=\Omega_0$ and $\omega=1+\omega_0$ when $\gamma=D+\gamma_0$. For model 1, when the period of the external potential $D \leqslant 2\gamma_1$ the phase diagram is similar to that of the standard FK model in appearance. The rotation numbers conform to the structure of Farey tree except for the case of $Q=1$, but the winding number do not increases montonically with the increasing of $\gamma$. For model 2, when the period of the external potential $D<2\gamma_2$, the phase diagram is similar to that of the standard FK model. When $D=2\gamma_2$, the phase diagram is very different. All the phases with $Q>1$ disappear when $K$ is greater than a threshold value $K_c$, where $K_c$ is approximate 4.0. For the two models, if $D$ is greater than the distance between the two minimum value points of $W(x)$, the $(K,\gamma)$ parameter space is divided into two unequivalent parts which cover the regions of $A_1:\gamma_1 \leqslant \gamma \leqslant D-\gamma_1$ and $A_2:D-\gamma_1 \leqslant \gamma \leqslant D+\gamma_1$, respectively, for model 1 or $B_1:\gamma_2 \leqslant \gamma \leqslant D-\gamma_2$ and $B_2:D-\gamma_2 \leqslant \gamma \leqslant D+\gamma_2$, respectively, for model 2. In the left part the diagram is similar to that of the standard FK model, and in the right part the phase diagram is identical to that in the case of $D=2\gamma_1$ or $D=2\gamma_2$. In the regions $A_1$ and $B_1$ the values of the winding number conform to the structure of the Farey tree. In the regions $A_2$ and $B_2$, the winging number $\omega=Q/Q$ when the rotation number $\Omega=P/Q$. When $\gamma<\gamma_1$ for model 1 or $\gamma<\gamma_2$ for model 2, $W(x)$ can not take its left minimum value, the phase diagram may be greatly different. The ground state $\{u_1,u_2,\ldots,u_Q\}$ obtained by using the effective potential method does not denote the real positions of the particles in the chain. The method for recovering the chain of the particles and calculating the winding number $\omega$ is given.

In conclusion, we emphasize that the new physics is that the systems of particles (not the spins) should be characterized by $U_n$, but in the process of calculation, one needs to rely on $u_n$. The two parameters redefined in this paper are also useful in the study on the modulated phases and the study on the phase diagram. The phase structures found in this paper are interesting. They contribute to a deeper understanding of the CI transitions and the FK-type models, espe-

cially the periodicity of the phase structures in the $(K,\gamma)$ parameter space. The mechanism for the occurrence of modulated phases and phase diagrams such as these may have potential applications in condensed-matter physics.

The method used in this paper can be applied to various versions of the generalized FK model with convex and nonconvex interparticle interactions.

The work of A. Xu, G. Wang, and S. Chen was supported by the National Natural Science Foundation of China and Science Foundation of China Academy of Engineering Physics, and that of B. Hu was supported in part by grants from the Hong Kong Baptist University (FGR) and the Hong Kong Research Grant Council (RGC).

*Electronic address: js8s@mail.iapcm.ac.cn

[1] For a review, see P. Bak, Rep. Prog. Phys. **45**, 587 (1982); T. Janssen and A. Janner, Adv. Phys. **36**, 519 (1987).

[2] T. Kontorova and Y. I. Frenkel, Zh. Éksp. Teor. Fiz. **8**, 89 (1938); **8**, 1340 (1938); **8**, 1349 (1938).

[3] S. Aubry, in *Solitons and Condensed Matter Physics*, edited by A. R. Bishop and T. Schneider (Springer-Verlag, New York, 1978), p. 264; M. Peyrard and S. Aubry, J. Phys. C **16**, 1593 (1983); S. Aubry, Physica D **7**, 240 (1983); S. Aubry and P. Y. Le Daeron, *ibid.* **8**, 381 (1983); L. de Seze and S. Aubry, J. Phys. C **17**, 389 (1984).

[4] S. N. Coppersmith and D. S. Fisher, Phys. Rev. B **28**, 2566 (1983).

[5] O. Biham and D. Mukamel, Phys. Rev. A **39**, 5326 (1989).

[6] B. Lin and B. Hu, J. Stat. Phys. **69**, 1047 (1992); J. Shi and B. Hu, Phys. Rev. A **45**, 5455 (1992); B. Hu, B. Lin, and J. Shi, Physica A **205**, 420 (1994).

[7] M. Marchand, A. Caille, and R. Pepin, Phys. Rev. B **34**, 4710 (1986).

[8] J. Villain and M. B. Gordon, J. Phys. C **13**, 3117 (1980).

[9] S. Little and A. Zangwill, Phys. Rev. B **46**, 7981 (1992).

[10] A. Banerjea and P. L. Taylor, Phys. Rev. B **30**, 6489 (1984).

[11] C. S. O. Yokoi, L. Tang, and W. Chou, Phys. Rev. B **37**, 2173 (1988).

[12] R. B. Griffiths and W. Chou, Phys. Rev. Lett. **56**, 1929 (1986); W. Chou and R. B. Griffiths, Phys. Rev. B **34**, 6219 (1986).

[13] M. Marchand, K. Hood, and A. Caille, Phys. Rev. Lett. **58**, 1660 (1987); Phys. Rev. B **37**, 1898 (1988).

[14] The models used in this paper are similar to those used in Ref. 13, but very different results are given.